Bezhenar, R., Maderich, V., Brovchenko, I., Boeira Dias, F. Äijälä, C., & Uotila, P. (2024). Lagrangian pathways connecting the Weddell and Bellingshausen Seas.
*Ukrainian Antarctic Journal*, *22*(2), 163–171.
https://doi.org/10.33275/1727-7485.2.2024.734





**Roman Bezhenar[1], Vladimir Maderich[1,*], Igor Brovchenko[1], Fabio Boeira Dias[2], Cecilia Äijälä[3], Petteri Uotila[3]**

[1] Institute of the Mathematical Machine and Systems Problems, Kyiv, 03187, Ukraine
[2] Climate Change Research Centre, University of New South Wales, Sydney, 2052, NSW, Australia
[3] Institute for Atmospheric and Earth System Research / Physics, Faculty of Science, University of Helsinki, Helsinki, 00100, Finland

*** Corresponding author:** vladmad@gmail.com

# Lagrangian pathways connecting the Weddell and Bellingshausen Seas

**Abstract.** This study assesses the connectivity of currents around the Antarctic Peninsula and identifies the structure of flows carrying virtual particles from the Eastern to Western Antarctic Peninsula continental shelves. We use circulation data for the Weddell and Bellingshausen Seas from the Whole Antarctica Ocean Model to obtain and analyse particle trajectories using the Probably A Really Computationally Efficient Lagrangian Simulator (Parcels) model. The software included the main Parcels kernels and a previously developed kernel that ensures the conservation of the number of particles during flow around irregularities in the bottom relief and the lower edge of ice shelves. We also developed a kernel to simulate convection in the ocean's upper mixed layer. Around 170000 virtual particles were released at a depth of 10 m during a year with a spatial step of 1° in two shelf and slope sectors in the southern Weddell Sea where the depth is less than 1500 m. The first sector covers the shelf area between 71°S and 77°S adjacent to the Filchner-Ronne Ice Shelf. The second sector covers the shelf area between 70°S and 65°S adjacent to the Larsen Ice Shelf. The pathways of water masses were characterised by the percentage of particles that visit each 10 × 10 km grid cell at least once in a modelling period of 20 years. 21% of particles cross 58°W (tip of the Antarctic Peninsula), while 70% of particles turn northeast. The smaller sector, adjacent to the Larsen Ice Shelf, is the main source of particles transferred to the Bellingshausen Sea (51%). In contrast, particles released in the larger sector were mostly transported to the northeast (75%). Only 3.4% of the released particles were transported to the west of 80°W, while the Amundsen Sea (105°W) was reached only by 0.1% of released particles. That indicates a virtual lack of circulation connectivity between the Weddell and the Amundsen Seas.

**Keywords:** Antarctic Peninsula, connectivity of ocean circulation, Parcels model, WAOM model

## 1 Introduction

The Southern Ocean's circulation specifics are determined primarily by the absence of a meridional boundary at the latitudes of the Drake Passage that results in the continuous ring of eastward currents around Antarctica (the Antarctic Circumpolar Current, ACC). In addition, there are westward currents on the shelf and continental slope. One of these is the Antarctic Slope Current (ASC), a band of water moving west along the continental slope. Another is the Antarctic Coastal Current (ACoC) flowing along the shelf's ice fronts and coastline. Shelf and slope topography, coastline geometry, buoyancy fluxes, and wind fields are key factors in forming these currents.

The Antarctic Peninsula (AP), which extends approximately 1300 km into the Southern Ocean, effectively separates the systems of shelf currents along its eastern and western coasts. In particular, the ASC disappears on both sides of the AP (Heywood et al., 2004; Thompson et al., 2018). The barrier effect and differences in topography lead to significant changes in the coastal circulation off the Western and Eastern Antarctic Peninsula (WAP and EAP, respectively). While the AP shields the currents on the Weddell Sea shelf from the effect of ACC, the currents on the Bellingshausen Sea shelf interact with the southern boundary of the ACC (Moffat & Meredith, 2018). The southern Weddell Sea shelf can be divided into a relatively narrow EAP shelf and a wide shelf with Filchner-Ronne Ice Shelf (FRIS). The WAP can be divided into the Bransfield Strait and the central WAP (Moffat & Meredith, 2018; Schubert et al., 2021).

The Bransfield Strait between the South Shetland Islands and the AP is a deep basin with a complicated cyclonic circulation pattern. The ACoC enters the Bransfield Strait around the AP tip, transporting about 1 Sv[1] (Heywood et al., 2004). Then it propagates along the Peninsula into the Bellingshausen Sea. Van Caspel et al. (2018) studied sources of water in the Bransfield Strait using the Finite Element Sea-ice Ocean Model (FESOM). Adding a passive tracer to the Glacial Melt Water (GMW), they found that GMW from FRIS has a larger influence on the Bransfield Strait bottom waters than the GMW from Larsen Ice Shelf. However, no evidence exists that this water reaches central WAP because the eastward current through the Gerlache Strait blocks it (Zhou et al., 2002). The Bransfield current flows oppositely along the South Shetland Islands (Sangra et al., 2011). Dawson et al. (2023) studied connectivity pathways from a circumpolar perspective using the ocean's general circulation model and Parcels, an offline Lagrangian particle trajectories model (Delandmeter & van Sebille, 2019). Specifying the source of particles on the Ronne shelf as a cross-section along 48°W, they found that 61% of the released particles reach the tip of the Antarctic Peninsula, while only 5% reach the shelf in West Antarctica.

In this paper, we used circulation data for the Weddell and Bellingshausen Seas from the Whole Antarctica Ocean Model (WAOM) (Richter et al., 2022) to obtain and analyse particle trajectories using Probably A Really Computationally Efficient Lagrangian Simulator (Parcels) model (Delandmeter & van Sebille, 2019). The analysis aims to assess the connectivity of currents around the AP and to identify the flow structures carrying particles from EAP to WAP shelves. Unlike Dawson et al. (2023), we consider a particle source spatially distributed over the shelf adjacent to the EAP to determine the area that is the main source of particles transferred from the Weddell Sea to the Bellingshausen Sea. The results of these Lagrangian simulations can also be used to plan and interpret measurements by floats and drifters.

## 2 Data and methods

### 2.1 WAOM

The WAOM circulation model was designed to describe ocean dynamics in the circum-Antarctica region (Richter et al., 2022). It is based on the Regional Ocean Modelling System (ROMS 3.6), a free-surface, terrain-following, primitive-equations ocean model that uses a curvilinear horizontal coordinate grid in south polar projection. The K-Profile-Parameterization (KPP) scheme (Large et al., 1994) parametrized vertical mixing, whereas harmonic viscosity and diffusivity were used to parametrize horizontal mixing. The thermodynamic interaction of the ice shelf and the ocean is described by the 3-equation model (Holland & Jenkins, 1999). Heat fluxes between air and sea based on satellite data (Tamura et al., 2011) were used instead of a dynamical-thermodynamical model for the sea ice. The boundary conditions at the lateral open boundaries are based on the reanalysis data from the ECCO2 modelling

[1] Sv (Sverdrup)=$10^6$ $m^3s^{-1}$

system (Menemenlis et al., 2008). The WAOM description and setup can be found in (Richter et al., 2022; Boeira Dias et al., 2023).

### 2.2 The Parcels model

The aim of a Parcels model (Delandmeter & van Sebille, 2019) is to compute Lagrangian particle trajectories using offline data produced by ocean general circulation models (OGCMs) containing fields of currents, temperature, salinity, and other parameters usually stored in different formats depending on the type of the OGCM. The movement of particles in the Parcels is simulated using interpolation schemes and special functions (kernels) responsible for particle dynamics.

The interpolation schemes are used to find OGCM water velocities, temperature, and salinity at a particle's location. They are described in (Delandmeter & van Sebille, 2019) for different types of OGCM grids. Kernels are used to calculate how particle position changes over time. There are several basic kernels for particle transport simulation due to advection and diffusion processes. One of the known problems of Lagrangian particle tracking is the loss of particles due to different reasons. Maderich et al. (2022) and Dawson et al. (2023) recently developed two kernels that recover particles. The first kernel recovers a particle in the last valid position with a small random variation in longitude, latitude, and depth. The kernel is applied until the particle continues its movement in the field of currents. In the second kernel, the particle is moved back from the coastline in a normal direction for a one-time step. The advantage of such recovering algorithms is that they ensure the conservation of the number of particles. We used the first kernel in the simulation.

A new kernel updated the particle tracking model to represent the convection, which was not explicitly described in the surface mixed layer. We followed the approach developed by van Sebille et al. (2013). In this approach, we defined the mixed layer depth as the layer where the potential density difference between the surface and a given depth

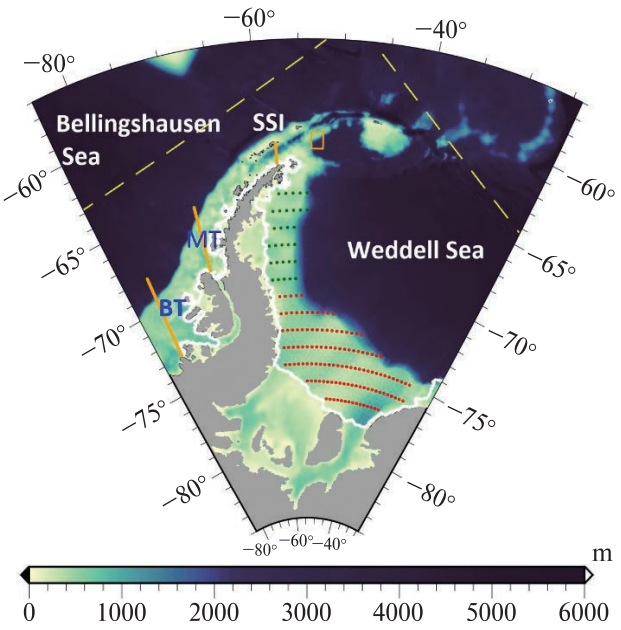


**Figure 1.** Map and the bathymetry of the Weddell and Bellingshausen Antarctic Peninsula sectors, showing ice shelves (white line). The scale shows the depth. Dots show the locations of particle release in the areas adjacent to the Ronne-Filchner (red) and Larsen (green) Ice Shelves. The dashed line shows the computational domain of the WAOM. Solid orange lines show cross sections at 58°, 70° and 80°W. The yellow quadrangle distinguishes particles carried by the Bransfield Current. SSI is the South Shetland Islands, MT is the Marguerite Trough, BT is the Belgica Trough

is less than 0.05 kg · $m^{-3}$. The profile of potential density for each time slice was calculated from the potential temperature and salinity. The convective mixing algorithm was applied when the particle appeared within the surface mixed layer. In that case, the particle jumped vertically over a distance calculated using the standard Python function Random. Uniform (−1.0, 1.0) with a maximum vertical velocity of 0.1 m · $s^{-1}$, which is the simple parameterisation of the random Brownian motion. There was no convective mixing below the mixed layer and under the ice shelf.

### 2.3 Modelling setup

A WAOM simulation's output (Boeira Dias et al., 2023) includes three components of velocity (*U*,

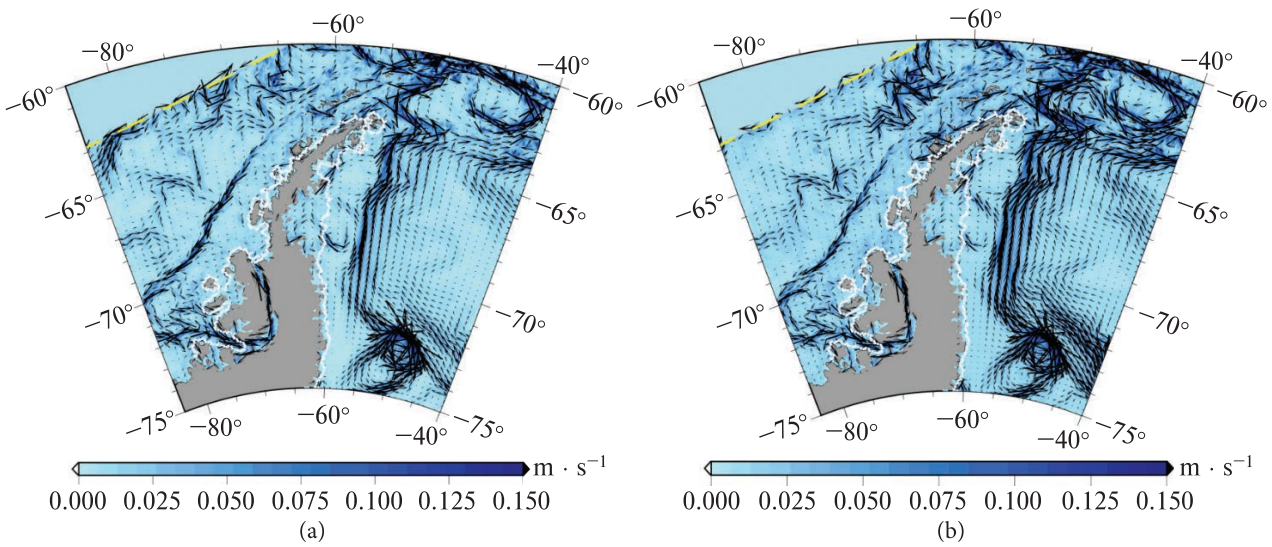


**Figure 2.** Depth-averaged velocities in the Weddell and Bellingshausen Antarctic Peninsula sectors in (a) summer (January, February, March) and (b) winter (July, August, September)

*V*, *W*), potential temperature (*T*), salinity (*S*), depth (*H*), sea level elevation (η), ice shelf draft ($z_{ice}$), horizontal coordinates for nodes of the computational grid (λ, φ), and vertical sigma-coordinates. The horizontal resolution of the grid was about 10 km. The vertical resolution was 32 levels. Timestep was 900 s (Richter et al., 2022; Boeira Dias et al., 2023). WAOM outputs were obtained after 20 years of spin-up simulations forced by repeated boundary conditions for the year 2007. This year was chosen because during it wind stress and buoyancy fluxes were the most non-anomalous compared to other available forcing years between 1992 and 2011 (Richter et al., 2022). Last-year data with the temporal resolution of 5 days were used as the output data set. For Lagrangian simulations, they were cycled (i.e., the yearly data were repeated).

Virtual particles were seeded every 8 hours during a year at 10 m below the surface with the spatial step of 1° of the longitude-latitude grid in two shelf and slope sectors where the ocean is shallower than 1500 m (Fig. 1). The first (red) sector covers a shelf area between 71°S and 77°S adjacent to the Filchner-Ronne ice shelf. The second (green) sector covers a shelf area between 70°S and 65°S adjacent to the Larsen ice shelf. This division allows us to estimate the contribution of the southern and northern sectors of the Weddell Sea shelf to the connectivity of circulation in the Weddell and Bellingshausen Seas. In total, 170 190 (137 250 red and 32 940 green) particles were released. The pathways of water masses were characterised by visitation frequency (Maderich et al., 2022). The 'visitation frequency' (Csanady, 1983) is the percentage of particles *P* that visit each 10 × 10 km grid cell at least once in a modelling period (20 years). When all particles visited the given area bin, $P = 100$; for no visits, $P = 0$.

The Parcels configuration used here includes random-walk kernels to describe winter convection and flow around the bottom relief, the lower surface of ice shelves, and the coast. Therefore, backtracking is not applicable here, unlike (Nissen et al., 2024), where convection processes were not taken into account. Instead, we identified and analysed only those trajectories that pass through the selected section. We identified the upstream paths and pinpointed the source regions by constructing the corresponding spatial distributions of visitation frequencies for trajectories that passed through this section. In general, the temperature

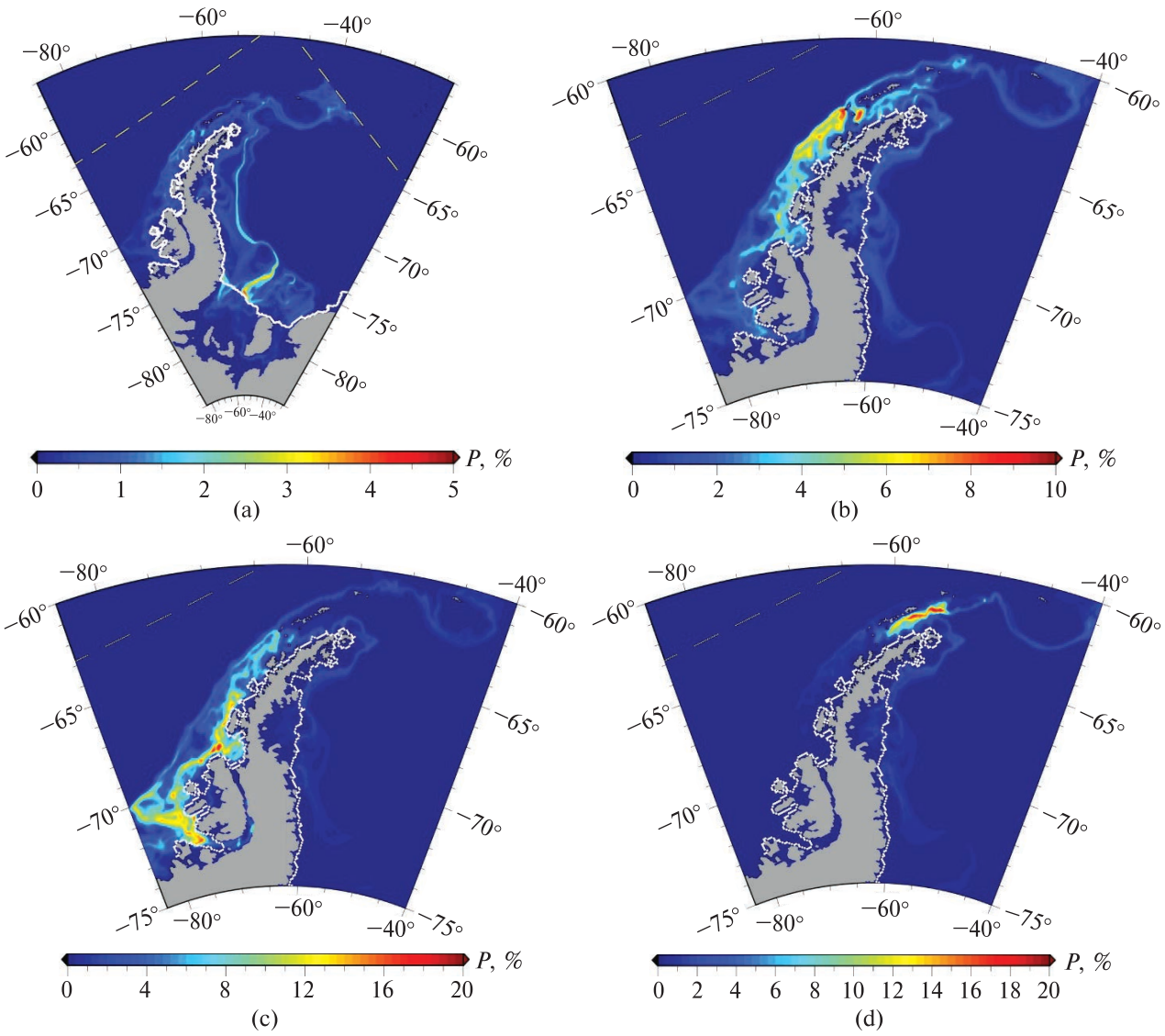


**Figure 3.** Visitation frequency $P$ [%] calculated for (a) all released particles on the Weddell Sea shelf; (b) for particles that crossed 58°W; (c) for particles that crossed 70°W; (d) for particles that crossed 58°W and the quadrangle in Figure 1 after that

and salinity can also be written along the virtual particle trajectory (see, e.g., Maderich et al., 2022). Here our task is to analyse the pathways of water masses; therefore, the transformation of particle properties is not considered.

## 3 Results

Figure 2 shows fields of depth-averaged velocities in the Weddell and Bellingshausen Antarctic Peninsula sectors in summer (January, February, March) (a) and winter (July, August, September) (b). As can be seen from the figure, the circulation in both seasons is qualitatively similar, although in winter, the currents are more intense. The dominant feature of circulation in the Weddell Sea is the ASC. It flows to the north, splitting into two branches at approximately 55°W. One branch turns to the Bransfield Strait flowing

along the AP, another turns to the east. The ACoC also turns to the Bransfield Strait. The Bransfield current directed to the northeast was reproduced in both seasons. The ASC again appeared along the WAP shelf break but higher up to the north than according to the analysis of shelf hydrography (Thompson et al., 2020).

The visitation frequency $P$ [%] calculated for all released particles on the Weddell Sea shelf is shown in Figure 3a. This figure demonstrates how particles released on the shelf propagate by currents toward the tip of AP. The distribution of visitation frequencies on the Weddell Sea shelf shows the presence of maxima corresponding to intense cross-shelf current flowing from beneath the Ronne Ice Shelf (RIS) and transporting ice shelf water (Maderich et al., 2022). In addition, in the western part of the RIS, water enters under the ice shelf and spreads beneath it and the Filchner Ice Shelf (FIS). A significant portion of the particles is transported by ASC along the shelf break to the north, after which the flux is split to the east and west. The eastward part of the flow corresponds to a deepening water mass – a precursor of Antarctic Abyssal Bottom Water. The splitting location agrees with the results of drifter experiments (Thompson et al., 2009).

As shown in the Table, the proportion of particles crossing 58°W is 21% of the total number of particles. Considering 9% of particles remained in the Weddell Sea, the proportion of particles turning northeast is 70%. These estimates differ from those obtained by Dawson et al. (2023), who found that 61% of the particles reach the tip of the Antarctic Peninsula. Such differences are explained by the fact that our particle source was distributed over the entire shelf of the southern Weddell Sea, whereas Dawson et al. (2023) distributed particles only over a single cross-section. Notably, the main source of particles transferred to the Bellingshausen Sea (51%) is the smaller green sector adjacent to the AP tip (Fig. 1). In contrast, 75% of particles released in the larger red sector were transported to the northeast, whereas 11% remained in the Weddell Sea. The particles remaining on the shelf are drawn into the circulation under the FRIS, accompanied by an outflow of water through the Hughes Trough to the Belgrano Bank, where a topographic eddy is formed (see Fig. 2). At the same time, almost all the particles seeded in the sector adjacent to the Larsen Ice Shelf left the source area. In addition, the seasonal distribution of the mixed layer thickness showed that winter convection covers the shelf and continental slope in the FRIS sector. In the shelf sector adjacent to the Larsen C Ice Shelf, the thickness of the mixed layer does not exceed several tens of meters due to the presence of freshened waters coming from the melting of the ice shelf (van Caspel et al., 2018). The eastward part of the flow corresponds to a deepening water mass – a precursor of Antarctic Abyssal Bottom Water. About 29% of all released particles dived below 1000 in the eastward flow, including 3 and 26% of green and red particles, respectively. At the same time, only 2% of released particles descended below 1000 m at 58°W equally from red and green release sectors. This means that pathways of particles strongly depend on the location from which these particles were released.

Figure 3b shows the distribution of visitation frequency for particles crossing 58°W. These particles move west along the WAP in the ACoC and then turn around to flow through the Bransfield

**Table.** Percentage of particle crossing cross-sections at the shelf of the Bellingshausen Sea

| Source sector | Remained in the Weddell Sea | 58°W | 70°W | 80°W | 105°W |
|---|---|---|---|---|---|
| Green | 0.04 | 51 | 20 | 8.4 | 0.3 |
| Red | 11 | 14 | 5.4 | 2.2 | 0.04 |
| Both | 9 | 21 | 8.4 | 3.4 | 0.1 |

Strait along the east coast of the South Shetland Islands. About 74% of particles flow in the upper 400 m layer. In this case, the contribution of green and red particles is approximately equal. Such a distribution indicates that the transport of ACoC is controlled by a relatively shallow coastal shelf at the AP tip. This issue requires further study, both with the help of floats and modelling with a higher spatial resolution. Only 8.4% of particles crossed 70°W. Figure 3c shows the distribution of visitation frequency for these particles, showing that most of them return to Drake Passage. These particles penetrate deep into the straits and bays of the WAP through the Marguerite and Belgica troughs, similar to drifters in experiments by Schubert et al. (2021). The farther to the west, the more particles are captured by the strong ACC. Thus, only 3.4% of the particles were transported west of 80°W, while only 0.1% reached the Amundsen Sea (105°W). This indicates a lack of connectivity between the circulation from the Weddell to the Amundsen Seas.

Figure 3d highlights the visitations of particles that first crossed 58°W moving to the west and later visited the sector between 52–53.5°W and 61.4–62.4°S, bounded by the quadrangle in Figure 1, at the north exit from the Bransfield Strait moving to the east. This made it possible to identify the path of the Bransfield Current along the western side of the South Shetland Islands. The U-turn of particles initially following the mainland coast of the WAP was also observed in the drifter experiments of Thompson et al. (2020). The drifters deployed east of the AP tip initially moved along the WAP, then turned north and east, forming the Bransfield Current at approximately 61°W by merging with the eastward current through the Gerlache Strait (Zhou et al., 2002).

## 4 Conclusions

The connectivity of currents around the AP and the structure of flows carrying particles from EAP to WAP shelves were studied using the WAOM and Parcels model output. In addition to the main Parcels kernels and a previously developed kernel that ensures the conservation of the number of particles in the flows around irregularities in the bottom relief and the lower edge of ice shelves, a new kernel was developed to represent convection in the upper mixed layer. The WAOM simulation used in this study was repeatedly forced by 2007 boundary conditions. This means that the model forcing does not consider interannual variability. Note that the parameterisation used for convective mixing implicitly considers the water column's stability. The virtual particles were released throughout the year with the spatial step of 1° in two shelf and slope sectors in the southern Weddell Sea. The proportion of particles crossing 58°W (the tip of the Antarctic Peninsula) is 21% of the total number of particles, while 70% turn northeast, and the proportion of remaining at shelf particles is 9%. The main source of particles transferred to the Bellingshausen Sea (51%) is the smaller sector adjacent to the Larsen ice shelf. In contrast, particles released in the larger sector adjacent to FRIS were mostly transported to the northeast (75%). Only 3.4% of the particles were transported west of 80°W, while the Amundsen Sea (105°W) was reached only by 0.1% of particles due to the continuous capturing of particles by strong ACC. This indicates a virtual lack of connectivity between the ocean circulation from the Weddell to the Amundsen Seas.

*Code availability.* The source code of the open-source Parcels model can be downloaded from github.com/OceanParcels/parcels. Installation instructions and detailed tutorials for working with the model are available on the website http://www.oceanparcels.org. The kernels developed by authors can be provided upon request.

*Author contributions.* V.M., P.U.: conceptualization. R.B., I.B.: numerical modeling. R.B., C.Ä., F.B.D.: data processing. V.M., I.B, C.Ä.: data analysis. V.M., R.B.: writing – original draft. I.B., F.B.D., P.U.: writing – review, and editing. All authors have read and agreed to the published version of the manuscript.

*Funding*: This work was supported by the European Union's Horizon 2020 research and innovation framework program (PolarRES, Grant Agreement 101003590) (C.Ä., P.U.), European Union's Horizon Europe Funding Programme for research and innovation (OCEAN:ICE, Grant Agreement no. 101060452) (R.B., V.M., I.B.), and the State Institution National Antarctic Scientific Center under the State Special-Purpose Research Program in Antarctica for 2011–2025 (R.B., V.M., I.B.).

*Conflict of Interest*. The authors declare that they have no conflict of interest.

**References**

Boeira Dias, F., Rintoul, S. R., Richter, O., Galton-Fenzi, B. K., Zika, J. D., Pellichero, V., & Uotila, P. (2023). Sensitivity of simulated water mass transformation on the Antarctic shelf to tides, topography and model resolution. *Frontiers in Marine Science, 10*, 1027704. https://doi.org/10.3389/fmars.2023.1027704

Csanady, G. T. (1983). Dispersal by randomly varying currents. *Journal of Fluid Mechanics, 132*, 375–394. https://doi.org/10.1017/S0022112083001664

Dawson, H. R. S., Morrison, A. K., England, M. H., & Tamsitt, V. (2023). Pathways and timescales of connectivity around the Antarctic continental shelf. *Journal of Geophysical Research: Oceans*, *128*(2), e2022JC018962. https://doi.org/10.1029/2022JC018962

Delandmeter, P., & van Sebille, E. (2019). The Parcels v2.0 Lagrangian framework: new field interpolation schemes. *Geoscientific Model Development, 12*(8), 3571–3584. https://doi.org/10.5194/gmd-12-3571-2019

Heywood, K. J., Naveira Garabato, A. C., Stevens, D. P., & Muench, R. D. (2004). On the fate of the Antarctic Slope Front and the origin of the Weddell Front. *Journal of Geophysical Research*, *109*(C6), C06021. https://doi.org/10.1029/2003jc002053

Holland, D. M., & Jenkins, A. (1999). Modeling thermodynamic ice-ocean interactions at the base of an ice shelf. *Journal of Physical Oceanography*, *29*(8), 1787–1800. https://doi.org/10.1175/1520-0485(1999)029<1787:MTIOIA>2.0.CO;2

Large, W. G., McWilliams, J. C., & Doney, S. C. (1994). Oceanic vertical mixing: A review and a model with a nonlocal boundary layer parameterization. *Reviews of Geophysics*, *32*(4), 363–403. https://doi.org/10.1029/94RG01872

Maderich, V., Bezhenar, R., Brovchenko, I., Bezhenar, A., Boeira Dias, F., & Uotila, P. (2022). Lagrangian pathways under the Filchner-Ronne Ice Shelf and in the Weddell Sea. *Ukrainian Antarctic Journal, 20*(2(25), 203–211. https://doi.org/10.33275/1727-7485.2.2022.700

Menemenlis, D., Campin, J., Heimbach, P., Hill, C., Lee, T., Nguyen, A., Schodlok, M., & Zhang, H. (2008). ECCO2: High resolution global ocean and sea ice data synthesis. In *American Geophysical Union Fall Meeting 2008*, OS31C-1292. https://ui.adsabs.harvard.edu/abs/2008AGUFMOS31C1292M/abstract

Moffat, C., & Meredith, M. (2018). Shelf–ocean exchange and hydrography west of the Antarctic Peninsula: a review. *Philosophical Transactions of the Royal Society. Series A, Mathematical, Physical, and Engineering Sciences*, *376*(2122), 20170164. https://doi.org/10.1098/rsta.2017.0164

Nissen, C., Timmermann, R., van Caspel, M., & Wekerle, C. (2024). Altered Weddell Sea warm- and dense-water pathways in response to 21st-century climate change. *Ocean Science*, *20*(1), 85–101. https://doi.org/10.5194/os-20-85-2024

Richter, O., Gwyther, D. E., Galton-Fenzi, B. K., & Naughten, K. A. (2022). The Whole Antarctic Ocean Model (WAOM v1.0): development and evaluation. *Geoscientific Model Development*, *15*(2), 617–647. https://doi.org/10.5194/gmd-15-617-2022

Sangrà, P., Gordo, C., Hernández-Arencibia, M., Marrero-Díaz, A., Rodríguez-Santana, A., Stegner, A., Martínez-Marrero, A., Pelegrí, J. L., & Pichon, T. (2011). The Bransfield current system. *Deep Sea Research Part I: Oceanographic Research Papers*, *58*(4), 390–402. https://doi.org/10.1016/j.dsr.2011.01.011

Schubert, R., Thompson, A. F., Speer, K., Schulze Chretien, L., & Bebieva, Y. (2021). The Antarctic Coastal Current in the Bellingshausen Sea. *The Cryosphere*, *15*(9), 4179–4199. https://doi.org/10.5194/tc-15-4179-2021

Tamura, T., Ohshima, K. I., Nihashi, S., & Hasumi, H. (2011). Estimation of surface heat/salt fluxes associated with sea ice growth/melt in the Southern Ocean. *SOLA*, *7*, 17–20. https://doi.org/10.2151/sola.2011-005

Thompson, A. F., Heywood, K. J., Thorpe, S. E., Renner, A. H. H., & Trasvica, A. (2009). Surface circulation at the tip of the Antarctic Peninsula from drifters. *Journal of Physical Oceanography*, *39*(1), 3–26. https://doi.org/10.1175/2008JPO3995.1

Thompson, A. F., Speer, K. G., & Schulze Chretien, L. M. (2020). Genesis of the Antarctic Slope Current in West Antarctica. *Geophysical Research Letters*, *47*(16), e2020GL087802.https://doi.org/10.1029/2020GL087802

Thompson, A. F., Stewart, A. L, Spence, P., & Heywood, K. J. (2018). The Antarctic Slope Current in a changing climate. *Reviews of Geophysics*, *56*, 741–770. https://doi.org/10.1029/2018RG000624

van Caspel, M., Hellmer, H. H., & Mata, M. M. (2018). On the ventilation of Bransfield Strait deep basins. *Deep*

*Sea Research Part II: Topical Studies in Oceanography, 149,* 25–30. https://doi.org/10.1016/j.dsr2.2017.09.006

van Sebille, E., Spence, P., Mazloff, M. R., England, M. H., Rintoul, S. R., & Saenko, O. A. (2013). Abyssal connections of Antarctic bottom water in a Southern Ocean state estimate. *Geophysical Research Letters*, *40*(10), 2177–2182. https://doi.org/10.1002/grl.50483

Zhou, M., Niiler, P. P., & Hu, J.-H. (2002). Surface currents in the Bransfield and Gerlache Straits, Antarctica. *Deep Sea Research Part I: Oceanographic Research Papers, 49*(2), 267–280. http://dx.doi.org/10.1016/s0967-0637(01)00062-0

Received: 26 September 2024
Accepted: 10 January 2025

**Роман Беженар[1], Володимир Мадерич[1,] *, Ігор Бровченко[1], Фабіо Боейра Діас[2], Сесилія Айяла[3], Петері Уотіла[3]**

[1] Інститут проблем математичних машин і систем НАН України, м. Київ, 03187, Україна
[2] Дослідницький центр змін клімату, університет Нового Південного Уельсу, м. Сідней, 2052, Австралія
[3] Інститут досліджень атмосферних і земних систем, університет Гельсінкі, м. Гельсінкі, 00100, Фінляндія

*** Автор для кореспонденції:** vladmad@gmail.com

**Лагранжеві шляхи, що з'єднують моря Ведделла і Беллінсгаузена**

**Реферат.** Це дослідження оцінює взаємозв'язок течій навколо Антарктичного півострова та визначає структуру потоків, що переносять віртуальні частинки зі східного на західний континентальний шельф Антарктичного півострова. Ми використовуємо дані про циркуляцію морів Ведделла та Беллінсгаузена з «Whole Antarctica Ocean Model», щоб отримати й проаналізувати траєкторії частинок за допомогою моделі «Probably A Really Computationally Efficient Lagrangian Simulator» (Parcels). Програмне забезпечення включало основні ядра Parcels і раніше розроблене ядро, яке забезпечує збереження кількості частинок під час обтікання нерівностей рельєфу дна і нижнього краю шельфового льодовика. Також ми розробили ядро для імітації конвекції у верхньому перемішаному шарі океану. Близько 170 000 віртуальних частинок було випущено на глибині 10 м протягом року з просторовим кроком 1° у двох секторах шельфу та континентального схилу в південній частині моря Ведделла, де глибина менше 1500 м. Перший сектор охоплює шельфовий район між 71° пд.ш. і 77° пд.ш., що прилягає до шельфового льодовика Фільхнера-Ронне. Другий сектор охоплює шельфовий район між 70° пд.ш. і 65° пд.ш., що прилягає до шельфового льодовика Ларсена. Шляхи руху водних мас характеризувались відсотком частинок, які відвідують кожну клітинку сітки 10 × 10 км принаймні один раз за період моделювання 20 років. 21% частинок перетинає 58° зх.д. (верхівка Антарктичного півострова), тоді як 70% частинок повертають на північний схід. Менший сектор, прилеглий до шельфового льодовика Ларсена, є основним джерелом частинок, що переносяться в море Беллінсгаузена (51%). На відміну від цього, частинки, випущені у більшому секторі, були здебільшого транспортовані на північний схід (75%). Лише 3.4% вивільнених частинок було перенесено на захід від 80° з.д., тоді як моря Амундсена (105° з.д.) досягли лише 0.1% вивільнених частинок. Це свідчить про фактичну відсутність зв'язку між циркуляцією в морях Ведделла та Амундсена.

**Ключові слова:** Антарктичний півострів, модель Parcels, модель WAOM, пов'язаність циркуляції